HIAS-E-127

High-frequency realized stochastic volatility model

Toshiaki Watanabe, Jouchi Nakajima

Hitotsubashi University

January 2023

Hitotsubashi Institute for Advanced Study, Hitotsubashi University
2-1, Naka, Kunitachi, Tokyo 186-8601, Japan
tel:+81 42 580 8668 http://hias.hit-u.ac.jp/

HIAS discussion papers can be downloaded without charge from:
https://hdl.handle.net/10086/27202
https://ideas.repec.org/s/hit/hiasdp.html

High-frequency realized stochastic volatility model*

Toshiaki Watanabe† and Jouchi Nakajima‡

January 2023

Abstract

A new high-frequency realized stochastic volatility model is proposed. Apart from the standard daily-frequency stochastic volatility model, the high-frequency stochastic volatility model is fit to intraday returns by extensively incorporating intraday volatility patterns. The daily realized volatility calculated using intraday returns is incorporated into the high-frequency stochastic volatility model by considering the bias in the daily realized volatility caused by microstructure noise. The volatility of intraday returns is assumed to consist of the autoregressive process, the seasonal component of the intraday volatility pattern, and the announcement component responding to macroeconomic announcements. A Bayesian method via Markov chain Monte Carlo is developed for the analysis of the proposed model. The empirical analysis using the 5-minute returns of E-mini S&P 500 futures provides evidence that our high-frequency realized stochastic volatility model improves in-sample model fit and volatility forecasting over the existing models.

Key words: Bayesian analysis, High-frequency data, Markov chain Monte Carlo, Realized volatility, Stochastic volatility model, Volatility forecasting.

*The authors thank the participants in the 4th International Conference on Econometrics and Statistics (EcoSta 2021), the Workshop "Macro- and Financial Econometrics" in the 7th Hitotsubashi Summer Institute (HSI 2021), and the 14th International Conference on Computational and Financial Econometrics (CFE 2020) for their valuable comments. The authors acknowledge financial support from the Ministry of Education, Culture, Sports, Science and Technology of the Japanese Government through Grant-in-Aid for Scientific Research No. 19H00588 (Watanabe only) and 20H00073, and Hitotsubashi Institute for Advanced Study.

†Center for the Promotion of Social Data Science Education and Research and Institute of Economic Research, Hitotsubashi University (E-mail: t.watanabe@r.hit-u.ac.jp).

‡Institute of Economic Research, Hitotsubashi University (E-mail: nakajima-j@ier.hit-u.ac.jp).

1 Introduction

Analysis of intraday time series of financial market variables has become popular and often provided richer information about price and volatility dynamics than traditional daily-frequency time series analysis. Realized volatility (RV) has been the main workhorse of this context and a wide range of methodological improvements and applications have been developed in the literature (e.g., Barndorff-Nielsen and Shephard, 2007; Andersen and Benzoni, 2009; Andersen et al., 2010). Compared to the traditional daily time series analysis with the stochastic volatility (SV) models (e.g., Ghysels et al., 2002; Shephard, 2005), the RV approach provides easily-computed measures of daily volatility based on the intraday price information for understanding price dynamics and forecasting volatility.

A hybrid approach that builds on the SV model with the RV measure is also proposed as the realized SV (RSV) models (e.g., Takahashi et al., 2009, 2016; Koopman and Scharth, 2012). The RSV model utilizes the daily RV in the context of daily SV models by formulating a measurement equation of the daily RV linked to the latent SV and microstructure noise. Takahashi et al. (2021) show that this modeling strategy improves the volatility forecasting performance of the daily SV model.

Stroud and Johannes (2014) shed light on the SV model in the context of high-frequency intraday time series, proposing a new approach that directly models the intraday returns in the form of traditional daily SV models but with practically relevant, intraday volatility patterns. The new model assumes that log-volatility of intraday (such as 5-min) returns follow a sum of persistent autoregressive processes and other key ingredients: seasonal components of the intraday volatility patterns and news announcement effects. These ingredients are commonly observed in intraday behaviors of stock returns. The seasonality of the intraday volatility pattern typically forms a U-shape, which characterizes relatively more volatile trading time at the opening and closing of trading hours. The stock market can be volatile at macroeconomic announcements such as releases of GDP estimates and of the central bank's monetary policy decisions. This news-effect component enriches the high-frequency SV model with respect to temporal hikes of the volatility following such announcements.

The current paper proposes a new high-frequency RSV model. We incorporate the daily RV calculated using intraday returns into the high-frequency SV model, considering the bias in the daily RV caused by microstructure noise. In line with the idea of the RSV models for daily returns, the daily RV in the proposed model is expected to

play an important role to pin down the latent variables of intraday SV. We apply the proposed model to the 5-minute returns of E-mini S&P 500 futures, following Stroud and Johannes (2014). We compare the proposed high-frequency RSV models with the high-frequency SV models to examine how introducing the daily RV works in the context of the high-frequency SV models. The empirical analysis provides evidence that our framework performs effectively in terms of model in-sample fit and volatility forecasting. The empirical results of in-sample fit and forecasting accuracy indicate that the proposed model dominates the high-frequency SV model.

As related literature, Bekierman and Gribisch (2021) propose a mixed-frequency intraday SV model, incorporating daily series of long-lived volatility factor and intraday series of short-lived volatility factors. The long-lived volatility factor is assumed as the latent variable which follows a simple AR(1) process evolving on a daily basis. In contrast, the current paper directly incorporates the daily RV with its measurement equation linked to the latent SV process structured in the high-frequency context to exploit the information in the daily RV for estimating the latent process and parameters in the high-frequency SV model. From another perspective, Santos (2019) uses trading volume to create a time-deformed series of intraday returns in the high-frequency SV models, based on the idea that increasing trading volume reflects more information arriving to the market, potentially yielding more changes in volatility.

The paper is organized as follows. Section 2 defines the high-frequency RSV models and discusses about each component of the proposed model. Section 3 describes the Bayesian computation for model fitting and forecasting. Section 4 provides an empirical analysis of the proposed models for E-mini S&P 500 futures. Finally, Section 5 concludes.

2 The model

2.1 High-frequency SV model

Define a univariate time series of high-frequency intraday return, $y_t = \log(P_t/P_{t-1})$, for $t = 1, 2, \ldots, T$, where P_t is the price at time t. The sampling frequency is seconds or minutes, such as 5 sec, 1 min, and 5 min. For the notation to describe both daily and intraday returns, let $y_{[k,\tau]}$ denote the return for the k-th intraday period on the day τ, for $k = 1, \ldots, K$, and $\tau = 1, \ldots, N$, where K is the number of intraday periods, and N is the number of days. This notation implies $y_{[1,1]} = y_1$, and $y_{[k,\tau]} = y_{k+(\tau-1)K}$.

For instance, as for the dataset of 5-min returns of E-mini S&P 500 futures used in the empirical analysis below, the time series covers the trading hours from 18:00 (EST) to 17:00 in each day with a short break from 16:15 to 16:30. In our intraday 5-min return series, we include two break-time returns from 16:15 to 16:30 and from 17:00 to 18:00. In sum, the number of intraday periods is $K = 275$. The data series continues from 18:00 on Sunday and to 17:00 on Friday, with a weekend trading closure from 17:00 on Friday to 18:00 on Sunday.

The return is modeled as

$$y_t \;=\; V_t \varepsilon_t + J_t Z_t, \qquad \varepsilon_t \;\sim\; \text{standardized } t(\nu), \tag{1}$$

where V_t is the total volatility, and $J_t Z_t$ is the jump component for returns.

The total volatility consists of three components:

$$V_t \;=\; X_t \cdot S_t \cdot A_t,$$

where X_t is the autoregressive factor of the SV, S_t is the intraday seasonal effect, and A_t is the announcement effect. Taking the log of the squared total volatility leads to

$$h_t \;\equiv\; \log(V_t^2) \;=\; x_t + s_t + a_t,$$

where $x_t = \log(X_t^2)$, $s_t = \log(S_t^2)$, and $a_t = \log(A_t^2)$. We describe the ingredients of the model in detail as follows.

Heavy-tailed errors

The heavy-tailedness of the error distribution is a well-known, important element in modeling stock returns with the daily SV models (e.g., Chib et al., 2002; Nakajima and Omori, 2009) and high-frequency intraday returns (e.g., Andersen et al., 2007, 2010). We incorporate the Student-t distribution with the degree-of-freedom ν, standardized such that the variance of ε_t is equal to one. Then, using the scale factor λ_t, we represent ε_t as

$$\varepsilon_t = \sqrt{\lambda_t}\epsilon_t, \quad \frac{\nu - 2}{\lambda_t} \sim \chi^2(\nu), \quad \epsilon_t \sim N(0,1), \text{ and } \nu > 2.$$

This formulation makes the posterior computation of the model easy and efficient with the latent variable λ_t. The distribution reduces to the normal distribution if ν is infinite.

For the model with normal errors, we set $\lambda_t = 1$, for all t.

SV autoregressive process

For the autoregressive process $\{x_t\}$, we specify a form of AR(1) model as

$$x_{t+1} = \mu + \phi(x_t - \mu) + \eta_t, \tag{2}$$

where

$$\begin{pmatrix} \epsilon_t \\ \eta_t \end{pmatrix} \sim N(\mathbf{0}, \boldsymbol{S}), \qquad \boldsymbol{S} = \begin{pmatrix} 1 & \rho\sigma \\ \rho\sigma & \sigma^2 \end{pmatrix}, \tag{3}$$

for $t = 1, \ldots, T-1$, and $x_1 \sim N(\mu, \sigma^2/(1-\phi^2))$, with $|\phi| < 1$. The leverage effect between the high-frequency intraday returns and volatility process is described by a negative correlation (ρ) between the shocks (ϵ_t, η_t) in Equation (3).

Stroud and Johannes (2014) assume that the SV component is the sum of two AR(1) processes to capture long- and short-lived autoregressive factors, by defining $x_t = x_{1t} + x_{2t}$, $x_{1,t+1} = \phi_1 x_{1t} + \eta_{1t}$, and $x_{2,t+1} = \mu + \phi_2(x_{2t} - \mu) + \eta_{2t}$, with $0 < \phi_2 < \phi_1 < 1$. This type of additive multi-process SV has been well studied and known as superposition models (e.g., Shephard, 1996; Omori et al., 2007). While Stroud and Johannes (2014) argue that the two autoregressive processes improve in-sample model fit and volatility forecasting over the single autoregressive process, Santos (2019) argues that estimating two autoregressive processes in the high-frequency SV model can be difficult to appropriately estimate even with strong priors and restriction on the parameters ($\phi_2 < \phi_1$), because the additive model of two similar latent processes could be too flexible to identify. We also encountered a situation that the MCMC algorithm does not safely converge when we formulate the two autoregressive models in our intraday SV and RSV models. For these reasons, we employ the single autoregressive process as above in this paper.

Jump component

Following a standard approach to modeling jumps in the context of daily SV models (Eraker et al., 2003; Chib et al., 2002; Nakajima and Omori, 2009), the jump component $J_t Z_t$ in Equation (1) is governed by the jump indicator variable, $J_t \in \{0, 1\}$, and the jump size denoted by Z_t. The jump occurs with the probability $0 < \kappa < 1$: $\Pr[J_t = 1] = \kappa$, for

$t = 1, \ldots, T$. We assume that the jump size follows the normal distribution:

$$Z_t \sim N(\mu_z, \sigma_z^2),$$

for $t = 1, \ldots, T$.

Stroud and Johannes (2014) formulate another jump component in the volatility equation (2), and assume that two jumps occur coincidently. We compared the model with jumps only in returns and the one with two coincident jumps and found that the jump in volatility has only a marginal gain for in-sample fit and out-of-sample forecasts. Therefore, we select the formulation without the jump in volatility for parsimonious modeling.

Intraday seasonal effect

Let β_k denote the intraday seasonal effect at intraday period k, for $k = 1, \ldots, K$. Define H_{tk} as an intraday-period indicator such that $H_{tk} = 1$, if time t corresponds to the period k, and zero otherwise. Then, the seasonal effect is specified by

$$\begin{aligned} s_t &= \sum_{k=1}^{K} H_{tk}\beta_k, \qquad t = 1, \ldots, T, \\ \beta_{k+1} &= \beta_k + \eta_{\beta,k}, \qquad \eta_{\beta,k} \sim N(0, c_k v_\beta^2), \qquad k = 1, \ldots, K-1. \end{aligned}$$

For the dynamics of the β_k process, Stroud and Johannes (2014) utilize a cubic smoothing spline. Alternatively, we propose the simple random-walk process to reduce a computational burden. Note that c_k denotes the time-varying part of the innovation variance. We set a large value for c_k for the time period k when we expect abrupt changes, such as an opening time of a local and a major international market, and set $c_k = 1$ for other k. To identify the latent processes and parameters, the formulation requires some restriction for $\{\beta_k\}$. Although Stroud and Johannes (2014) propose the restriction, $\frac{1}{K}\sum_{k=1}^{K}\beta_k = 0$, and use an ad-hoc sampling step to satisfy it, this approach makes an exact sampling scheme intractable. In the current paper, we instead define $\beta_1 = 0$.

Announcement effects

We consider the announcement effect for each macroeconomic announcement $j = 1, \ldots, J$, where J denotes the number of announcements. Let $\alpha_{j\ell}$ denote the effect of announcement j at ℓ periods after the news release, for $\ell = 1, \ldots, L$. We set $L = 24$, which

means that each announcement can impact on the volatility up to 2 hours after the announcement in case of 5-min returns. Further, define $I_{jt\ell}$ as an announcement-period indicator such that $I_{jt\ell} = 1$, if time t corresponds to the period ℓ after the announcement j, and zero otherwise. Then, the announcement effect is specified by the first-order autoregressive process, that is,

$$\begin{aligned} a_t &= \sum_{j=1}^{J}\sum_{\ell=1}^{L} I_{jt\ell}\alpha_{j\ell}, \qquad t = 1, \ldots, T, \\ \alpha_{j,\ell+1} &= \varphi_j \alpha_{j\ell} + \zeta_{j\ell}, \qquad \zeta_{j\ell} \sim N(0, v_{\alpha j}^2), \qquad \ell = 1, \ldots, L-1, \end{aligned}$$

where $|\varphi_j| < 1$, for $j = 1, \ldots, J$. For modeling the announcement effect, Stroud and Johannes (2014) use the cubic smoothing spline. For the same reason mentioned above, we instead employ the simple autoregressive process to reduce a computational burden.

2.2 High-frequency RSV model

We introduce the daily series of RV to propose the high-frequency RSV model. A plain RV is defined as

$$\mathrm{RV}_\tau = \sum_{k=1}^{K} y_{[k,\tau]}^2, \quad \tau = 1, \ldots, N. \tag{4}$$

In our empirical analysis, we compute this RV using 5-min returns only when the market is open, i.e., excluding break-time returns.

A key equation in our high-frequency RSV model is the measurement of the RV:

$$\log(\mathrm{RV}_\tau) = \xi + \log \sum_{t \in D(\tau)} \exp(h_t) + u_\tau, \quad u_\tau \sim N(0, \sigma_u^2), \tag{5}$$

for $\tau = 1, \ldots, N$, where $D(\tau)$ denotes a set of intraday time points on Day τ. The parameter ξ addresses the bias in the RV. If $\xi = 0$, $\log(\mathrm{RV}_\tau)$ is an unbiased estimator of the log of the true daily volatility, $\log \sum_{t \in D(\tau)} \exp(h_t)$.

This equation connects the RV calculated using intraday returns to the model-implied true volatility with the bias correction. The RSV model for daily returns (Takahashi et al., 2009; Koopman and Scharth, 2012) links the daily RV with the daily model-implied volatility. In line with this idea, it could be effective to connect an intraday (say, 5-min) RV to intraday model-implied volatility, $\exp(h_t)$, in the high-frequency RSV model.

However, such an intraday RV is difficult to compute properly due to the microstructure noise. Therefore, we come up with daily RV for the link in the measurement equation of our high-frequency RSV model. Another frequency (i.e., a half day) to compute the RV may also work, which we will discuss later as future work.

Assume that $p(t)$, denoting the log of an asset price, follows a jump-diffusion process:

$$dp(t) = \mu(t)dt + \sigma(t)dW(t) + \kappa(t)dN(t), \tag{6}$$

where t is continuous time, $\mu(t)$ is drift, $\sigma(t)$ is instantaneous volatility, $\kappa(t)$ is the jump size, and $N(t)$ is counting measure. If $p(t)$ does not include noise,

$$\operatorname*{plim}_{K\to\infty} \mathrm{RV}_\tau = \int_{\tau-1}^{\tau} \sigma^2(t)dt + \sum_{\tau-1<t\leq\tau} \kappa^2(t)dt. \tag{7}$$

The first term of the right-hand side is called the integrated volatility or continuous component, which corresponds to $\sum_{t\in D(\tau)}\exp(h_t)$. The second term is called the jump component. There are some methods available for separating RV_τ into the estimate of the continuous component, $\hat{C}_\tau$ and that of the jump component $\hat{J}_\tau$ (Barndorff-Nielsen and Shephard, 2004, 2006; Corsi et al., 2010). Strictly speaking, equation (5) should be replaced by

$$\begin{aligned}
\log(\hat{C}_\tau) &= \xi_1 + \log \sum_{t\in D(\tau)} \exp(h_t) + u_{1,\tau}, \quad u_{1,\tau} \sim N(0, \sigma_1^2), \\
\log(1+\hat{J}_\tau) &= \xi_2 + \log\left(1 + \sum_{t\in D(\tau)} (J_t Z_t)^2\right) + u_{2,\tau}, \quad u_{2,\tau} \sim N(0, \sigma_2^2).
\end{aligned}$$

Since it makes the estimation difficult, we simply use equation (5), so that the jump component is included in ξ and u_τ in equation (5).

3 Bayesian analysis and computation

3.1 Model estimation

Based on observation $\boldsymbol{y} \equiv (y_1, \ldots, y_T)$, we consider model fitting using the Bayesian MCMC methods including conditional samplers for each model component. The al-

gorithm is implemented with collections of the samplers for the daily SV models with leverage, jumps, and heavy-tailed errors (Chib et al., 2002; Omori and Watanabe, 2008; Nakajima and Omori, 2009) and for the state space dynamic models (e.g., Prado and West, 2010).

The full set of posterior computations consists of the following conditional samplers for latent processes and model parameters:

1. The latent autoregressive SV process: $\boldsymbol{x} \equiv (x_1, \ldots, x_T)$.
2. The jump components: $\boldsymbol{J} \equiv (J_1, \ldots, J_T)$ and $\boldsymbol{Z} \equiv (Z_1, \ldots, Z_T)$.
3. The intraday seasonal and announcement effects: $\boldsymbol{\beta} \equiv (\beta_1, \ldots, \beta_K)$ and $\boldsymbol{\alpha} = \{\boldsymbol{\alpha}_1, \ldots, \boldsymbol{\alpha}_J\}$, where $\boldsymbol{\alpha}_j \equiv (\alpha_{j1}, \ldots, \alpha_{jL})$, for $j = 1, \ldots, J$.
4. The mixing latent process: $\boldsymbol{\lambda} \equiv (\lambda_1, \ldots, \lambda_T)$.
5. The parameters defining the latent SV process: $\boldsymbol{\theta}_X \equiv (\phi, \sigma, \rho, \mu)$.
6. The jump parameters: $\boldsymbol{\theta}_J \equiv (\kappa, \mu_z, \sigma_z)$.
7. The parameters defining the intraday seasonal and announcement effects: $\boldsymbol{v} \equiv (v_\beta, v_{\alpha 1}, \ldots, v_{\alpha J})$ and $\boldsymbol{\varphi} \equiv (\varphi_1, \ldots, \varphi_J)$.
8. The degree of freedom for the Student-t distribution: ν.
9. The parameters defining the RV measurement equation: (ξ, σ_u)

This algorithm generates samples from the full posterior distribution $\pi(\boldsymbol{\psi}, \boldsymbol{\theta}|\boldsymbol{y})$, where $\boldsymbol{\psi} = \{\boldsymbol{x}, \boldsymbol{J}, \boldsymbol{Z}, \boldsymbol{\lambda}\}$, and $\boldsymbol{\theta} = \{\boldsymbol{\beta}, \boldsymbol{\alpha}, \boldsymbol{\theta}_X, \boldsymbol{\theta}_J, \boldsymbol{v}, \boldsymbol{\varphi}, \nu, \xi, \sigma_u\}$. Details of the MCMC computation are documented in Appendix.

Stroud and Johannes (2014) employ the so-called mixture sampler developed by Kim et al. (1998), and Omori et al. (2007) in their MCMC algorithm for the high-frequency SV model. The main challenge to generating the posterior sample from the SV model is the nonlinearity of the return equation in terms of volatility. Kim et al. (1998) take the logarithm of both sides of the equation to make the model linear and approximate the log chi-squared distribution by a normal mixture distribution. Conditional on an auxiliary variable associated with the mixture distribution, the model reduces to a linear Gaussian state space representation, and we can apply an efficient sampler such as the simulation smoother (e.g., de Jong and Shephard, 1995). Although it is well known that

an approximation error is negligible (Omori et al., 2007), Stroud and Johannes (2014) mix up the mixture sampler and other conditional samplers based on the exact model specification. Therefore, the current paper proposes the exact algorithm fully based on the original model representation using the efficient multi-move sampler (Shephard and Pitt, 1997; Omori and Watanabe, 2008).

3.2 Model evaluation

For the model comparison exercises, we consider in-sample fit and out-of-sample forecasts. This subsection describes methods to compute measures for the model comparison.

3.2.1 In-sample fit

In a Bayesian framework, we can compare models based on a posterior probability that is proportional to the product of the prior probability of the model and the marginal likelihood. A Bayes factor, which is the ratio of two posterior probabilities, is often used to measure he relative degree of in-sample fit. However, a computation of the marginal likelihood requires considerable a computation burden when the model includes many parameters. Therefore, we instead calculate the BIC, which is a good approximation of the Bayes factor when the number of observations is quite large as in our analysis.

The likelihood of the proposed high-frequency RSV model is estimated using the auxiliary particle filter (e.g., Pitt and Shephard, 1999; Chib et al., 2002; Omori et al., 2007; Stroud and Johannes, 2014). Define $\boldsymbol{Y}_t \equiv (y_1, \ldots, y_t)$, as the data up to time t. The likelihood of the high-frequency RSV model for $\boldsymbol{Y}_T$ is given by

$$L(\boldsymbol{Y}_T \,|\, \boldsymbol{\theta}) \;=\; \prod_{t=0}^{T-1} f(y_{t+1} \,|\, \boldsymbol{\theta}, \boldsymbol{Y}_T),$$

where the right-hand side of this equation is the product of the predictive density:

$$f(y_{t+1} \,|\, \boldsymbol{\theta}, \boldsymbol{Y}_t) \;=\; \int p(y_{t+1} \,|\, \boldsymbol{\theta}, \boldsymbol{Y}_t, \boldsymbol{\psi}_{t+1}) \cdot p(\boldsymbol{\psi}_{t+1} \,|\, \boldsymbol{\theta}, \boldsymbol{Y}_t) d\boldsymbol{\psi}_{t+1},$$

where $\boldsymbol{\psi}_t = (x_t, \lambda_t, J_t, Z_t)$. In the auxiliary particle filter, we use the posterior mean $\hat{\boldsymbol{\theta}}$ estimated by the MCMC algorithm to approximate the likelihood density.

To compute the BIC, let L_i and d_i denote the likelihood and the number of parameters

in Model i. The BIC for Model i is defined by $\text{BIC}_i = -2\log L_i(\boldsymbol{Y}_T|\hat{\boldsymbol{\theta}}) + d_i \log(T)$. The second term of this criterion is the penalty for a more flexible model that includes more parameters. Note that we treat $\boldsymbol{\beta}$ and $\boldsymbol{\alpha}$ as the parameters in $\boldsymbol{\theta}$, making them fixed at their posterior means in the auxiliary particle filter, and also counting them in the number of parameters (d_i).

3.2.2 Out-of-sample volatility forecasting

To compare the out-of-sample fit among competing models, we conduct a recursive forecasting exercise based on one-day-ahead daily volatility forecast. Given the data up to day τ, we run the MCMC algorithm and generate $\boldsymbol{\psi}_{[k,\tau+1]}$, $y_{[k,\tau+1]}$, and $V_{[k,\tau+1]}$, for $k = 1, \ldots, K$, at each MCMC iteration. The resulting posterior predictive density of these variables reflects parameter uncertainty in the specified model. Let $\sigma^2_{\tau+1}$ and $\widehat{\sigma}^2_{\tau+1}$ denote the true volatility and the volatility forecast for day $\tau + 1$, respectively. We compute the quadratic variation as the forecast of one-day-ahead volatility:

$$\widehat{\text{QV}}^{(i)}_{\tau+1} = \sum_{k=1}^{K} (y^{(i)}_{[k,\tau+1]})^2, \quad \text{and} \quad \widehat{\sigma}^2_{\tau+1} = \frac{1}{I}\sum_{i=1}^{I} \widehat{\text{QV}}^{(i)}_{\tau+1},$$

where (i) and I denote the i-th iteration of the MCMC algorithm and the total number of iterations, respectively, and $y^{(i)}_{[k,\tau+1]}$ denotes a draw from the posterior predictive distribution of $y_{[k,\tau+1]}$ at the i-th iteration. We run the MCMC algorithm to estimate model parameters and latent variables and to obtain the one-day-ahead volatility forecast for each business day. We recursively conduct this computation every business day for the forecasting period.

Stroud and Johannes (2014) use the particle filtering method to obtain the out-of-sample forecast with all the parameters fixed in their forecasting exercise. In contrast, we conduct the rolling estimation with MCMC sampling and obtain the posterior predictive mean as a point forecast. Note that our method takes account uncertainty in the parameters.

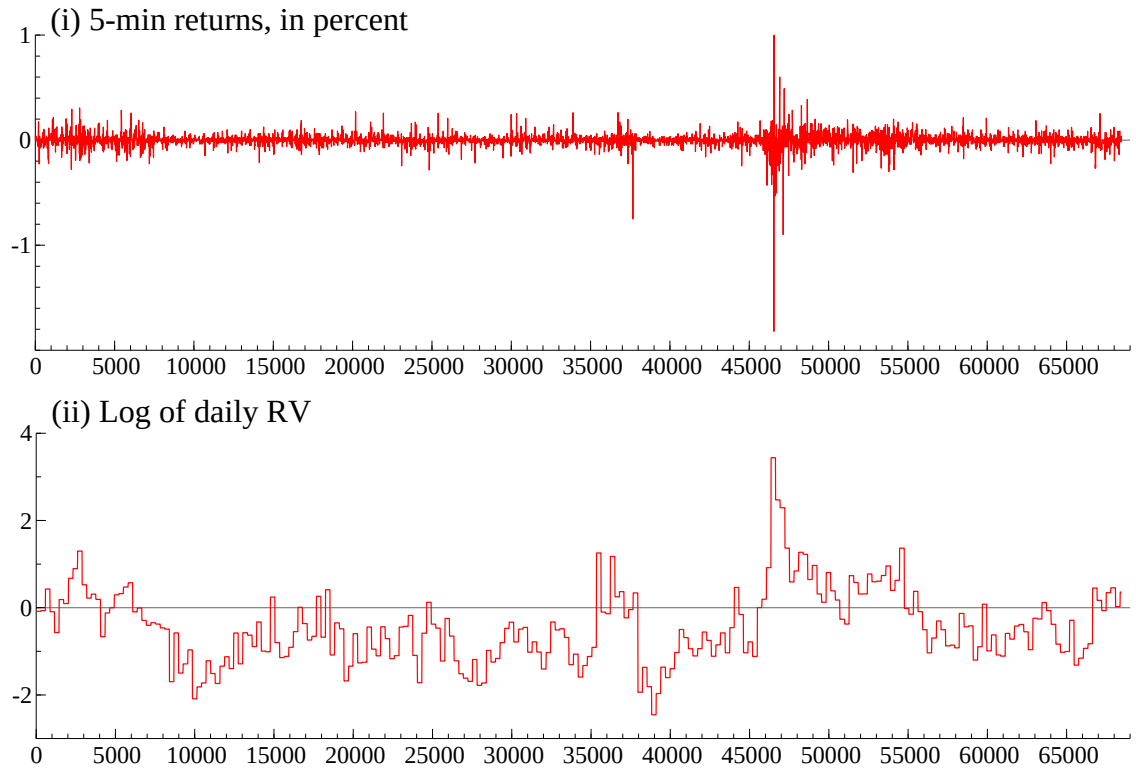

Figure 1: 5-min intraday returns (top) and log of daily RV (bottom) of E-mini S&P 500 futures from January 1 to December 31 in 2015. The RV series is plotted in a step function with the intraday 5-min frequency.

4 Empirical analysis

4.1 Data and setup

The high-frequency RSV model is fit to 5-min intraday returns of E-mini S&P 500 futures, which are traded on the Chicago Mercantile Exchange's Globex platform. As mentioned above, our dataset covers the prices from 18:00 (EST) on Sunday and to 17:00 on Friday, for 24 hours including two breaks from 16:15 to 16:30 and 17:00 to 18:00. We count each business day from 18:00 to 18:00, and create 5-min return series including two break-time returns to obtain $K = 275$ intraday returns. The sample period spans from January 1, 2015, to December 31, 2019. We divide this sample period into the first year and the rest four years as the pre-analysis and the forecasting exercise periods, respectively. The number of business days is $N = 249$ and 996 for these two periods, respectively. The whole sample is $N = 1{,}245$ and $T = 342{,}375$.

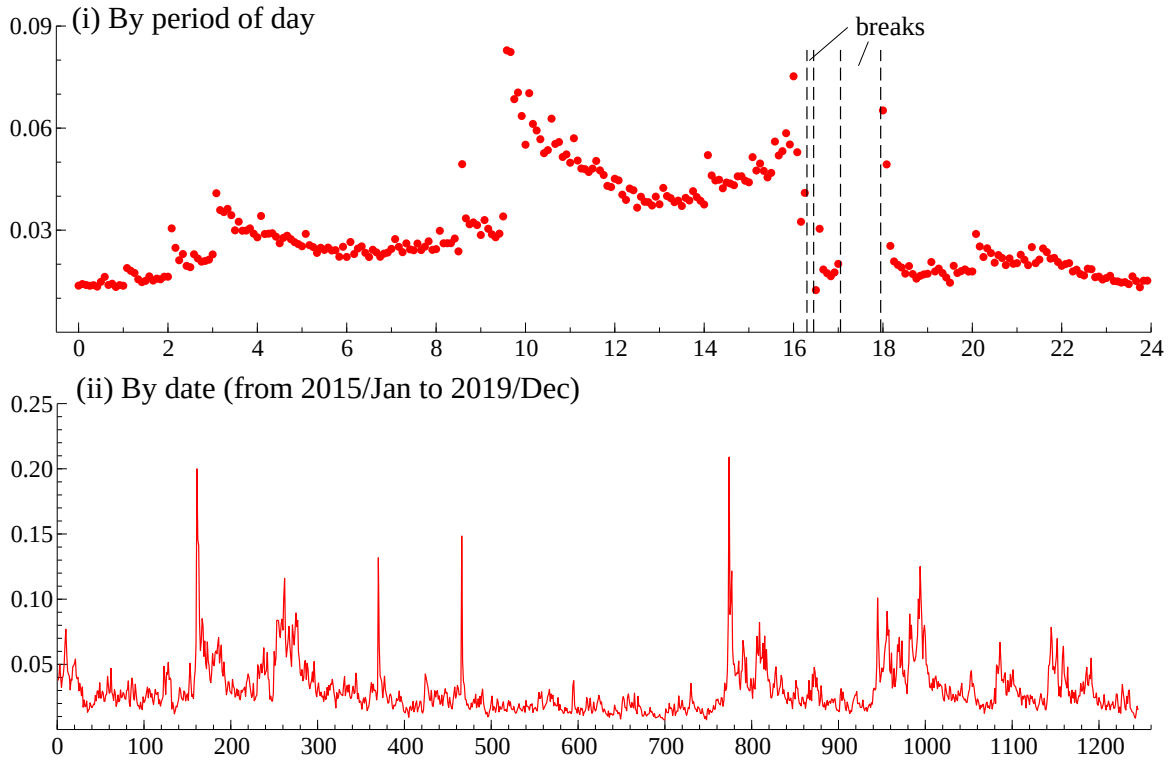

Figure 2: Standard deviations of 5-min intraday returns of E-mini S&P 500 futures in percent, by the period of day (top) and by date (bottom) for the full sample period, from January 1, 2015, to December 31, 2019. In the top panel, the horizontal axis shows an hour during the day in EST.

Figure 1 plots the 5-min intraday returns for the pre-sample period, which shows considerably time-varying volatility. It also plots the daily RV calculated using the 5-min intraday returns. It markedly hikes in the second half of the sample, reflecting a high volatility period as in the top panel. To illustrate *intraday* and *interday* volatility patterns, Figure 2 plots the standard deviation of returns ($y_{[k,\tau]}$) by the period of day (horizontal for $k = 1, \ldots, K$) and by date (for $\tau = 1, \ldots, N$), which are computed using the full-sample period. The intraday pattern in the top panel highlights some hikes which mostly reflect openings in international financial markets. That is, we find small hikes at 3:00, 4:00, 20:00, when Frankfurt, London, and Hong Kong markets open, respectively, and a relatively larger increase at 9:30, corresponding to the opening of the New York market. During the New York trading hours that end at 16:00, we observe a U-shaped pattern where the prices tend to be more volatile around the opening and closing times.

Table 1 reports summary statistics for the intraday returns in the pre-analysis and

Period	Mean	Stdev.	Skewness	Kurtosis	Min.	Max.
(a) 2015/Jan – 2015/Dec	0.000	0.061	-0.543	84.40	-1.819	2.160
(b) 2016/Jan – 2019/Dec	0.000	0.052	-1.061	87.48	-3.067	1.328

Table 1: Summary statistics for 5-min intraday returns of E-mini S&P 500 futures, in percent, for the (a) pre-analysis period ($N = 259$, $T = 68{,}475$) and (b) forecasting exercise period ($N = 996$, $T = 273{,}900$).

1	ADP Employment (monthly)
2	Consumer Price Index (monthly)
3	Durable Goods (monthly)
4	GDP Advance Estimate (quarterly)
5	Monthly Payrolls (monthly)
6	Empire State Manufacturing (monthly)
7	Consumer Confidence (monthly)
8	Philadelphia Fed Manufacturing Index (monthly)
9	ISM Manufacturing Index (monthly)
10	ISM Services Index (monthly)
11	FOMC Minutes (twice a quarter)
12	FOMC Announcements (twice a quarter)

Table 2: Macroeconomic statistics for announcements effect.

forecasting exercise periods. For both periods, the skewness is negative, and the kurtosis is remarkably high. This fact implies that the 5-min return distribution has considerably heavy tails. We examine how the leverage effects, heavy-tailed errors, and jumps capture these characteristics of high-frequency intraday stock returns.

For the Bayesian inference, the following priors are used: $(\phi+1)/2 \sim B(20, 1.5)$, $\sigma^2 \sim IG(40, 0.2)$, $(\rho+1)/2 \sim B(1,1)$, $\mu \sim N(-5, 1)$, $\nu \sim G(16, 0.8)I[\nu > 2]$, $\kappa \sim B(1, 500)$, $\mu_z \sim N(0,1)$, $\sigma_z^2 \sim IG(20, 4)$, $\xi \sim N(0,1)$, $\sigma_u^2 \sim IG(2.5, 0.025)$, $v_\beta^2 \sim IG(40, 1)$, $\beta_2 \sim N(0, 100)$, $v_{\alpha j}^2 \sim IG(40, 1)$, $\alpha_{j1} \sim N(0, 100)$, and $(\varphi_j + 1)/2 \sim B(10, 1.5)$, for $j = 1, \ldots, J$, where B and G denote the beta and gamma distributions, respectively. From the observation of the intraday volatility pattern in Figure 2, we set $c_k = 100$ for $k = 1, 25, 109, 121, 187, 265, 271$, which correspond to the opening and closing time of relevant international financial markets mentioned above, including the times 16:30 and 18:00, which corresponds to the time after the breaks of S&P E-mini futures trading. For the daily series of RV, we calculate it using the 5-minute returns only for trading hours as explained above.

For the macroeconomic announcements, we use releases of major economic statistics and Federal Reserve Boards' announcements listed in Table 2, which are the same as used by Stroud and Johannes (2014) with one exception that we exclude Jobless Claims as its announcement effects are statistically not relevant in our high-frequency SV and RSV models, through the pre-sample and forecasting exercise periods. We assume $J = 24$, which implies the announcement effects can be alive for 2 hours after the announcement. Following Stroud and Johannes (2014), we include Sunday opens as it tends to be volatile responding to information gathered during the weekend. Note that we do not take into account how different the released number of the macroeconomic statistics or contents of the policy announcements is, compared to market expectations. It is reasonable to consider that the larger the "market surprise" is, the higher the volatility gets. Examining the relationship between the market surprise and volatility is of interest, which is left as future work.

The MCMC analysis was run for a burn-in period of 2,000 samples prior to saving the following 20,000 samples. We use every fifth draw of them for the posterior inferences. To check the convergence of the MCMC algorithm, we compute the convergence diagnostic (CD) of Geweke (1992). With the MCMC sample size specified here, the resulting CDs indicate that the null hypothesis that the Markov chain converges is not rejected at a 5 percent statistical significance level in our analysis. The computational results are generated using Ox version 7.0 (Doornik, 2006).

In the following analysis, the following four types of high-frequency RSV models are considered:

- **RSV:** normal distribution, no jumps ($\lambda_t = 0$ and $J_t = 0$, for all t);
- **RSVt:** Student t-distribution, no jumps ($J_t = 0$, for all t);
- **RSVJ:** normal distribution, with jumps in return ($\lambda_t = 0$, for all t);
- **RSVJt:** Student t-distribution, with jumps in return.

All the models described here include the leverage effect, the intraday volatility pattern, and the macroeconomic announcement effects. For each formulation above, we consider the high-frequency SV model, which excludes the measurement equation of the daily RV.

	RSV	RSVJ	RSVt	RSVJt
ϕ	0.981 (0.001) [0.979, 0.983] 13.2	0.986 (0.001) [0.984, 0.989] 24.0	0.989 (0.001) [0.987, 0.990] 10.7	0.989 (0.001) [0.988, 0.991] 16.1
σ	0.219 (0.008) [0.198, 0.229] 26.3	0.182 (0.009) [0.160, 0.194] 28.2	0.160 (0.003) [0.154, 0.164] 23.0	0.157 (0.006) [0.143, 0.166] 31.0
ρ	-0.064 (0.013) [-0.087, -0.040] 2.3	-0.100 (0.014) [-0.129, -0.076] 3.1	-0.106 (0.016) [-0.134, -0.079] 9.2	-0.112 (0.015) [-0.142, -0.082] 3.2
μ	-7.641 (0.185) [-7.856, -7.248] 42.4	-6.301 (0.094) [-6.481, -6.138] 23.2	-7.287 (0.091) [-7.440, -7.102] 22.3	-5.566 (0.390) [-6.324, -5.041] 47.3
v_β	0.252 (0.016) [0.225, 0.287] 11.6	0.244 (0.015) [0.219, 0.274] 1.2	0.304 (0.028) [0.255, 0.349] 34.9	0.241 (0.013) [0.219, 0.269] 0.4
$v_{\alpha 1}$	0.313 (0.052) [0.234, 0.435] 1.2	0.305 (0.041) [0.232, 0.393] 2.6	0.310 (0.045) [0.231, 0.408] 2.5	0.311 (0.050) [0.236, 0.441] 1.0
φ_1	0.896 (0.104) [0.625, 0.998] 2.3	0.891 (0.111) [0.600, 0.996] 1.1	0.832 (0.146) [0.470, 0.996] 3.2	0.854 (0.190) [0.280, 1.000] 0.7
κ		0.0032 (0.0005) [0.0023, 0.0044] 13.9		0.0005 (0.0002) [0.0002, 0.0009] 25.2
μ_z		-0.005 (0.022) [-0.050, 0.039] 0.4		-0.072 (0.114) [-0.307, 0.140] 3.3
σ_z		0.264 (0.024) [0.223, 0.313] 8.7		0.412 (0.044) [0.340, 0.514] 8.0
ν			7.672 (0.588) [6.912, 8.946] 46.4	8.673 (0.654) [7.942, 10.152] 41.2
ξ	-0.078 (0.012) [-0.101, -0.055] 2.8	-0.036 (0.014) [-0.059, -0.004] 2.2	-0.119 (0.016) [-0.163, -0.093] 11.4	-0.113 (0.015) [-0.139, -0.061] 23.4
σ_u	0.109 (0.009) [0.093, 0.128] 4.3	0.139 (0.014) [0.115, 0.166] 8.8	0.159 (0.015) [0.134, 0.193] 2.7	0.164 (0.015) [0.137, 0.195] 2.9

The first row: posterior mean and standard deviation in parentheses.
The second row: 95% credible interval in square brackets.
The third row: inefficiency factor.

Table 3: Posterior estimates of the selected parameters for the high-frequency RSV models for E-mini S&P 500 futures, obtained from the pre-sample period: January 1 to December 31 in 2015 ($N = 259$ and $T = 68{,}475$).

4.2 Posterior estimates

Table 3 reports the posterior estimates of selected parameters for the high-frequency RSV models fit to the pre-analysis period. Note that for $v_{\alpha j}$ and ψ_j, we report their first elements ($j = 1$). The posterior mean of the AR(1) coefficient ϕ in the latent SV process indicates a considerable persistence, ranging from 0.98 to 0.99. The posterior means of (ϕ, σ) are $(0.981, 0.219)$ for the RSV model, while $(0.989, 0.157)$ for the RSVJt model. The latter model includes heavier tails of the error distribution and jump components, which makes the autoregressive component more persistent with a smaller variance.

The posterior mean of ρ is around -0.1, with the credible intervals excluding zero, which indicates that the leverage effect exists as commonly observed for the daily stock return and volatility. The posterior mean of ν, estimated around 8, indicates that the error distribution requires considerably heavy tails. In the jump models, the posterior mean of κ is about 0.3% for the RSVJ model and 0.05% model for the RSVJt model. The lower probability of jumps in the RSVJt model implies that some large returns in absolute value are captured by the heavy-tailed error distribution. For the same reason, the posterior mean of σ_z for the RSVJt model is higher than that for the RSVJ model as estimated jumps are averagely larger in the RSVJt model than the RSVJ model.

For the parameters in the measurement equation of the RV, the posterior mean of ξ is from -0.119 to -0.036 with the credible intervals excluding zero, which indicates that the bias underlying the measurement equation is negative. The bias in RV caused by microstructure noise can be positive or negative (Hansen and Lunde, 2005). As mentioned above, we use the RV calculated using intraday returns only when the market is open, while the model-implied true daily volatility is a whole day's (24-hour's) volatility, which causes a negative in RV. The estimation result suggests that the negative bias derived from non-trading hours dominates.

The table also reports the inefficiency factor to check the efficiency of the MCMC algorithm. This factor is defined by $1 + 2\sum_{s=1}^{\infty} \rho_s$ where ρ_s is the sample autocorrelation at lag s, estimating the ratio of the numerical variance of the posterior sample mean to the variance of the sample mean from uncorrelated draws, as a measure of how well the MCMC chain mixes (see, e.g., Chib, 2001). We compute the inefficiency factor using a Parzen window with bandwidth $b_w = 1{,}000$. The resulting inefficiency factors are all less than 100, which is as modest as for the standard SV models for daily stock returns. This result indicates that the MCMC algorithm developed in this paper mixes well enough to

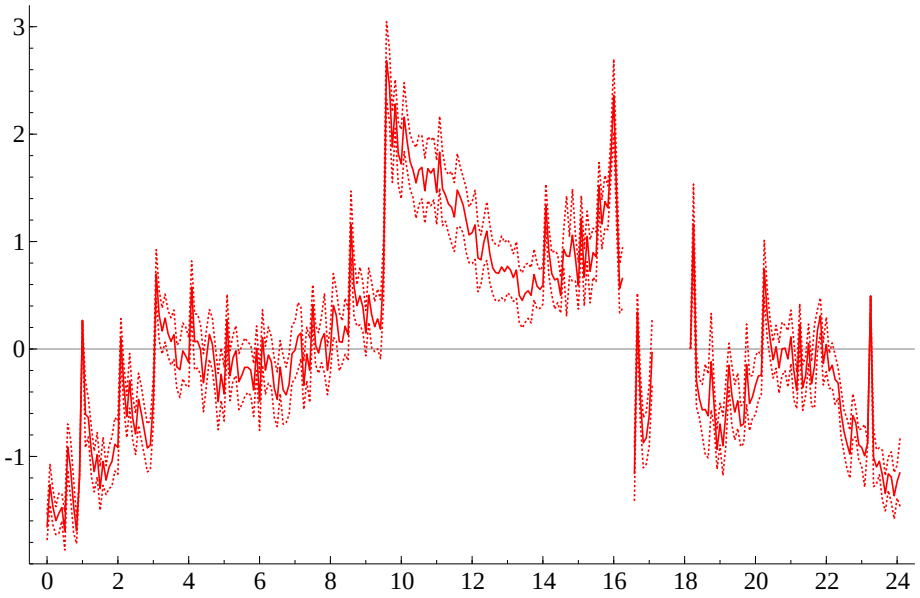

Figure 3: Intraday volatility pattern: posterior means (solid) and 95% credible intervals (dotted) for the volatility intraday seasonal effects $(\beta_1, \ldots, \beta_K)$, obtained from the RSVJt model for the pre-analysis period. The horizontal axis shows an hour during the day in EST. Breaks of market trading occur from 16:00 to 16:15 and from 17:00 to 18:00.

be practically applied to the real-data analysis.

Figure 3 shows the posterior estimates for the intraday volatility pattern with the posterior mean and 95% credible intervals of $\boldsymbol{\beta}$, obtained from the RSVJt model. The result shows a marked intraday pattern of volatility, which shifts up from 9:30 to 16:00 reflecting the trading hours of the New York market. The credible intervals are quite narrow, which suggests that this intraday pattern is empirically relevant.

Figure 4 plots the posterior estimates for the macroeconomic announcement effects, which indicate that the influence of releases of CPI and Employment are statistically important for the intraday volatility. While the effects of the other announcements seem to be modest, we find that the effects change over time as some of them become significant, with the credible intervals excluding zero when the estimation period is changed. For the impact of Sunday open, the posterior estimate suggests it should be distinguished.

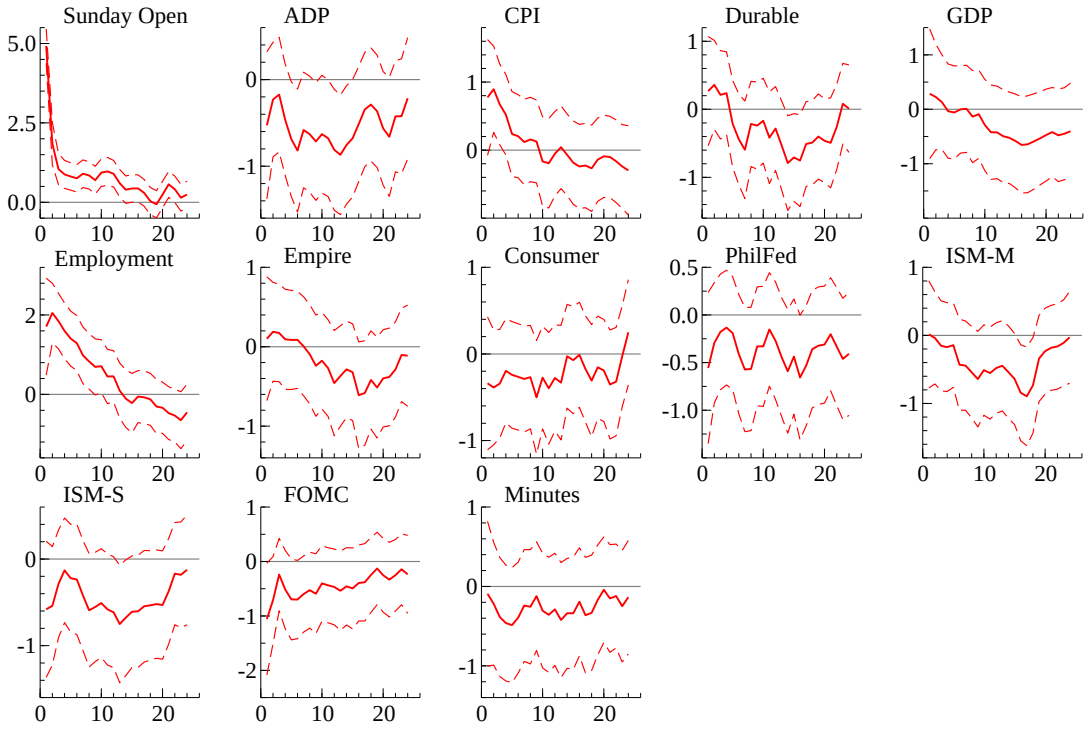

Figure 4: Macroeconomic announcement effects: posterior means (solid) and 95% credible intervals (dashed) of $\alpha_{j\ell}$, obtained from the RSVJt model for the pre-analysis period.

4.3 Model comparisons

4.3.1 Result of in-sample fit

Table 4 reports the estimated BICs for the high-frequency SV and RSV models obtained from the full sample period. Due to a computational burden, we fit the competing models to the data separately in each calendar year from 2015 to 2019 and sum them up. Because the high-frequency RSV models specify the additional measurement equation of the daily RV, we use a partial likelihood only for the measurement of intraday returns (y_t) in the high-frequency RSV models to compare the in-sample fit between the high-frequency SV and RSV models.

The estimated BIC indicates that using daily series of RV improves the in-sample fit. Based on the BIC, the RSVJt model is the best model, and the RSVt model is the second among the competing models. In the class of the high-frequency RSV model, the model with Student t-error distribution (RSVt and RSVJt) fits the data better than that with the normal error distribution (RSV and RSVJ).

Model	BIC	MSE	QLIKE
RSV	-682037 [6]	2.198 [6]	0.748 [3]*
RSVJ	-678130 [7]	2.048 [3]*	0.763 [4]*
RSVt	-693029 [2]	1.937 [1]*	0.718 [2]*
RSVJt	-696145 [1]	1.951 [2]*	0.702 [1]*
SV	-683399 [5]	2.352 [8]	0.821 [8]
SVJ	-677555 [8]	2.325 [7]	0.782 [7]*
SVt	-683883 [4]	2.089 [4]	0.774 [6]*
SVJt	-692880 [3]	2.179 [5]	0.774 [5]*

Table 4: Result of model comparison: BIC for in-sample model fit, and MSE and QLIKE for one-day-ahead volatility forecasts. The sample period is 2015/Jan to 2019/Dec (N = 1,245) for BIC and 2016/Jan to 2019/Dec (N = 996) for MSE and QLIKE. Rankings are in square brackets. The model with the "*" mark is in the 90% model confidence set (MCS).

4.3.2 Result of out-of-sample forecast performance

We compare the predictive ability of one-day-ahead volatility among the competing models, based on the mean squared error (MSE) and quasi likelihood (QLIKE) as loss functions, following Patton (2011):

$$\text{MSE} = \frac{1}{N_1}\sum_{\tau=N_0+1}^{N_0+N_1}\left(\widehat{\text{QV}}_\tau^2 - \text{QV}_\tau^2\right)^2, \quad \text{QLIKE} = \frac{1}{N_1}\sum_{\tau=N_0+1}^{N_0+N_1}\left(\frac{\text{QV}_\tau^2}{\widehat{\text{QV}}_\tau^2} + \log\widehat{\text{QV}}_\tau^2\right).$$

Since the true QV is unobserved, we must use the proxy. Patton (2011) shows that the MSE and QLIKE are robust loss functions in the sense that they lead to the same ranking as the one when the true volatility is used if the proxy is the unbiased estimator of the true volatility. In our analysis, we calculate the RV using 30-min returns, including the break-time returns.

In our out-of-sample forecasting exercise, we employ a rolling-window forecasting strategy. First, we estimate the model using data for $N_0 = 249$ business days, which corresponds to the pre-analysis period, January 1 to December 31, 2015, and forecast the volatility on the next business day, January 3, 2016. Next, we roll the data window by one business day with the sample size kept the same ($N = 249$) and forecast the one-day-ahead volatility. We repeat this procedure until all the data are used in the

forecasting exercise period, which ends on December 31, 2019. In sum, we obtain the forecasted volatility for $N_1 = 996$ business days.

Table 4 reports the MSE and QLIKE obtained from the forecasting exercise. The MSE and QLIKE suggest that the RSVt and RSJt models provide the best performance of volatility forecasting, respectively. The class of high-frequency RSV models is uniformly better than that of high-frequency SV models based on both measures. The models with Student t-error distribution perform better than those with the normal error distribution. The influence of introducing the jump component on the predictive ability is marginal, based on the MSE and QLIKE.

To evaluate the MSE and QLIKE further, we compute the model confidence set (MCS) proposed by Hansen et al. (2011). Following Takahashi et al. (2021), the MCS is estimated with $1,000$ bootstrap replications and 10 blocks, using R package `MCS`. In Table 4, the models indicated by the "*" mark are in the 90% MCS. Based on QLIKE, the SV model is excluded for the best set of models. Based on MSE, all the specifications without the RV are excluded, and the MCS consists of the RSVJ, RSVt, and RSVJt models.

To further assess whether the difference in QLIKE is critical in the model comparison, we examine the hypothesis testing proposed by Giacomini and White (2006), which we call the GW tests hereafter. For two candidate models i and j, we define $d_{ij,t}$ as a loss difference on the day t. Giacomini and White (2006) propose two types of hypothesis tests, unconditional and conditional.

To test equal unconditional predictive ability, the following null hypothesis is considered:

$$\mathrm{H}_0 : \quad \mathrm{E}[d_{ij,t}] \, = \, 0, \quad \forall i, j \in M_1, \quad i > j.$$

The test statistics for this null hypothesis are computed with the Newey-West heteroscedasticity and autocorrelation consistent estimator.

The conditional predictive ability is examined using the following null hypothesis:

$$\mathrm{H}_0 : \quad \mathrm{E}[d_{ij,t+1}|I_t] \, = \, 0,$$

where I_t is the information set up to the day t. This hypothesis testing bases the expected loss difference between two models on the day $t+1$ given the information up to the day t. Following Takahashi et al. (2021), we define $\boldsymbol{q}_t = (1, d_{ij,t})'$ and arrange the null hypothesis

Model	SVt	SVJt	RSVt	RSVJt
SVt		0.46*	0.89*	0.93**
SVJt	−0.03		1.00*	1.00**
RSVt	−2.00**	−2.57**		0.68*
RSVJt	−2.74**	−3.70**	−0.83	

Table 5: Result of model comparison in the GW tests for the QLIKE loss function. Lower triangular elements: the test statistics (t-value) of the unconditional GW tests; upper triangular elements: the proportion for which the row model has higher predicted losses than the column model on the conditional GW tests. Values with the "**" and "*" marks indicate the statistical significance with the 1% and 5% levels, respectively.

as

$$\mathrm{H}_0 : \quad \mathrm{E}[\boldsymbol{q}_t d_{ij,t+1}] = 0.$$

See Takahashi et al. (2021) for the computation of the test statistics for this hypothesis.

Table 5 reports the test statistics of the unconditional GW tests in the lower triangular elements, where a positive value indicates that the row model has a higher loss than the column model. The table also reports, in its upper triangular elements, the proportion for which the row model has higher predicted losses than the column model on the conditional GW tests. Here, we compare only the candidate models with t-distribution because these are mostly superior to the normal-error models in the analyses above. Evidently, the RSVt and RSVJt models perform better than the SVt and SVJt models because both the unconditional and conditional GW tests indicate that the null hypotheses are rejected with the 1% significance level. The result for the difference in QLIKE between the RSVt and RSVJt models is mixed. The conditional GW test indicates that the RSVJt model is superior to the RSVt model with 5% statistical significance, while the unconditional GW test does not reject the null hypothesis.

5 Conclusion

This paper proposes the high-frequency RSV model for intraday stock returns. The model consists of the latent autoregressive SV process, seasonal components of the intraday volatility patterns, and jumps in prices. The key aspect of the proposed model is to

specify the measurement equation of RV, which links the daily RV and model-implied true volatility with the bias of microstructure noise taken into account. We apply the proposed model to the 5-min returns of E-mini S&P 500 futures and show that the daily RV plays an important role in describing the intraday volatility. The model comparison exercise indicates that the daily RV improves both the in-sample fit and performance of one-day-ahead volatility forecasting.

Although we specify the daily frequency for the RV series, another frequency, such as half-day, may also work. From the finding that the intraday volatility gets relatively higher during the trading hours of the New York market, the RV computed using only the intraday returns during these hours may be more relevant for the measurement equation in the high-frequency RSV model. We leave this point as future work. From another perspective, we can extend the high-frequency RSV model by incorporating a skewed error distribution. It is of interest to investigate how the skewed distribution capture the heavy tails and asymmetry of the return distribution (e.g., Takahashi et al., 2016; Nakajima, 2017), which is relevant in volatility forecasting and risk management analysis.

Appendix. MCMC algorithm for the high-frequency RSV model

In this appendix, we document details of the MCMC computation method for the high-frequency RSV model, which is outlined in Section 3.1.

A.1 Stochastic volatility process

We derive a posterior sampler for the latent SV process $\boldsymbol{x}$, conditional on other state processes and parameters. Defining $y_t^* = (y_t - J_t Z_t) \exp\{-(\mu + s_t + a_t)/2\}/\sqrt{\lambda_t}$, and $\tilde{x}_t = x_t - \mu$, we obtain a non-linear state-space model:

$$\begin{aligned} y_t^* &= \exp(\tilde{x}_t/2)\epsilon_t, \\ \tilde{x}_{t+1} &= \phi\tilde{x}_t + \eta_t, \\ \log(\mathrm{RV}_\tau) &= \xi + \log \sum_{t \in D(\tau)} \exp(\tilde{x}_t + \mu + s_t + a_t) + u_\tau, \end{aligned}$$

where $(\epsilon_t, \eta_t)' \sim N(\mathbf{0}, \boldsymbol{S})$, and $\tilde{x}_1 \sim N(0, \sigma^2/(1-\phi^2))$. We assume that ϵ_t (or η_t) and u_τ are uncorrelated for any t and τ. To implement the conditional sampler for $(\tilde{x}_1, \ldots, \tilde{x}_T)$, we arrange the multi-move sampler for the SV model with leverage (Omori and Watanabe, 2008).

A.2 Jump component

Define $\hat{y}_t = y_t - \sqrt{\lambda_t} r_t e^{h_t/2}$, $r_t = \rho_t(\tilde{x}_{t+1} - \phi\tilde{x}_t)/\sigma$, $w_t^2 = \lambda_t(1-\rho_t^2)e^{h_t}$, where $\rho_t = \rho \cdot I[t < T]$, for $t = 1, \ldots, T$; and $I[\,\cdot\,]$ denotes the indicator function that takes one, if the argument is true, and zero otherwise. Conditional on $(\boldsymbol{y}, \boldsymbol{x}, \boldsymbol{\theta}_X, \boldsymbol{\theta}_J, \boldsymbol{\beta}, \boldsymbol{\alpha})$, the joint conditional posterior density of the jump indicator and size can be written as

$$\pi(J_t, Z_t \,|\, \cdot\,) \;\propto\; \exp\left\{-\frac{(\hat{y}_t - J_t Z_t)^2}{2w_t^2} - \frac{(Z_t - \mu_z)^2}{2\sigma_z^2}\right\} \times \kappa^{J_t}(1-\kappa)^{1-J_t},$$

for $t = 1, \ldots, T$. Integrating this joint posterior density with respect to Z_t, we obtain

$$\begin{aligned}\pi(J_t \,|\, \cdot\,) \;&\propto\; \int \pi(J_t, Z_t \,|\, \cdot\,) dZ_t \\ &\propto\; (w_t^2 + \sigma_z^2 J_t)^{-1/2} \exp\left\{-\frac{(\hat{y}_t - J_t\mu_z)^2}{2(w_t^2 + \sigma_z^2 J_t)}\right\} \times \kappa^{J_t}(1-\kappa)^{1-J_t}.\end{aligned}$$

We generate the sample of J_t, following the posterior jump probability

$$\Pr[J_t = 1 \,|\, \cdot\,] \;=\; \frac{\kappa \cdot \phi_N\left(\hat{y}_t \,|\, \mu_z,\, w_t^2 + \sigma_z^2\right)}{(1-\kappa) \cdot \phi_N\left(\hat{y}_t \,|\, 0,\, w_t^2\right) + \kappa \cdot \phi_N\left(\hat{y}_t \,|\, \mu_z,\, w_t^2 + \sigma_z^2\right)},$$

for $t = 1, \ldots, T$, where $\phi_N(\hat{y}_t \,|\, \mu, \sigma^2)$ denotes the density function of a normal distribution $N(\mu, \sigma^2)$ at $\hat{y}_t$.

Given the jump indicator, the posterior distribution of the jump size is given by

$$Z_t \,|\, (J_t = 1) \;\sim\; N(\hat{\mu}_t,\, \hat{\sigma}_t^2),$$

where

$$\hat{\sigma}_t^2 = \left(\frac{1}{w_t^2} + \frac{1}{\sigma_z^2}\right)^{-1}, \quad \text{and} \quad \hat{\mu}_t \;=\; \hat{\sigma}_t^2\left(\frac{\hat{y}_t}{w_t^2} + \frac{\mu_z}{\sigma_z^2}\right),$$

for $t = 1, \ldots, T$.

A.3 Intraday seasonal and announcement effects

Define $\tilde{h}_t = x_t + a_t$. The conditional posterior distribution of $\boldsymbol{\beta}$ is given by

$$\begin{aligned}
\pi(\boldsymbol{\beta}\,|\,\cdot) &\propto \pi(\boldsymbol{\beta}\,|\,v_\beta) \times \prod_{t=1}^{T} \frac{1}{e^{s_t/2}} \exp\left\{ -\frac{(y_t - \sqrt{\lambda_t} r_t e^{(\tilde{h}_t + s_t)/2} - J_t Z_t)^2}{2\lambda_t(1-\rho_t^2) e^{\tilde{h}_t + s_t}} \right\} \\
&\propto \pi(\boldsymbol{\beta}\,|\,v_\beta) \times \prod_{k=1}^{K} \prod_{H_{tk}=1} \frac{1}{e^{\beta_k/2}} \exp\left\{ -\frac{(y_t - \sqrt{\lambda_t} r_t e^{\tilde{h}_t/2} e^{\beta_k/2} - J_t Z_t)^2}{2\lambda_t(1-\rho_t^2) e^{\tilde{h}_t} e^{\beta_k}} \right\} \\
&\propto \pi(\boldsymbol{\beta}\,|\,v_\beta) \times \prod_{k=1}^{K} \frac{1}{e^{N\beta_k/2}} \exp\left\{ -\frac{\sum_{H_{tk}=1} (\tilde{y}_t^* - g_t e^{\beta_k/2})^2}{2e^{\beta_k}} \right\},
\end{aligned}$$

where

$$\tilde{y}_t^* = \frac{y_t - J_t Z_t}{\sqrt{\lambda_t(1-\rho_t^2)} e^{\tilde{h}_t/2}}, \qquad g_t = \frac{r_t}{\sqrt{1-\rho_t^2}}.$$

It leads to the following non-linear state space model:

$$\begin{aligned}
\tilde{y}_{[k,\tau]}^* &= g_{[k,\tau]} e^{\tilde{\beta}_k/2} + e^{\tilde{\beta}_k/2} \varepsilon_{[k,\tau]}, \quad k = 1, \ldots, K,\ \tau = 1, \ldots, N, \\
\beta_{k+1} &= \beta_k + \eta_{\beta,k}, \quad k = 1, \ldots, K-1, \\
\begin{pmatrix} \varepsilon_{[k,\tau]} \\ \eta_{\beta,k} \end{pmatrix} &\sim N(\mathbf{0},\, \boldsymbol{V}_k), \qquad \boldsymbol{V}_k = \begin{pmatrix} 1 & 0 \\ 0 & c_k v_\beta^2 \end{pmatrix},
\end{aligned}$$

where $\beta_1 = 0$, and $\eta_{\beta,1} \sim N(0, v_{\beta 0}^2)$. We apply the multi-move sampler for the non-linear state space model (Shephard and Pitt, 1997; Watanabe and Omori, 2004) to generate $\boldsymbol{\beta}$. The announcement effect $\boldsymbol{\alpha}$ is sampled by the multi-move sampler in the same manner by defining $\tilde{h}_t = x_t + s_t$.

A.4 Mixing latent process

The conditional posterior density of λ_t is

$$\pi(\lambda_t\,|\,\cdot) \propto \lambda_t^{-\frac{\nu+1}{2}-1} \exp\left(-\frac{\nu-2}{2\lambda_t}\right) \times f(\lambda_t),$$

where

$$f(\lambda_t) \;=\; \exp\left\{-\frac{(y_t - \sqrt{\lambda_t} r_t e^{h_t/2} - J_t Z_t)^2}{2\lambda_t(1-\rho_t^2)e^{h_t}}\right\}.$$

The MH algorithm is employed to generate λ_t. We generate a candidate as $\lambda_t^* \sim IG((\nu+1)/2, (\nu-2)/2)$, and accept it the with probability: $\min\{f(\lambda_t^*)/f(\lambda_t),\, 1\}$, for $t = 1, \ldots, T$.

A.5 SV parameters

For the SV parameter ϕ, let $\pi(\phi)$ denote the prior distribution. The conditional posterior density of ϕ is

$$\begin{aligned}
\pi(\phi\,|\,\cdot) \;&\propto\; \pi(\phi)\sqrt{1-\phi^2}\exp\left\{-\frac{(1-\phi^2)\tilde{x}_1^2}{2\sigma^2} - \sum_{t=1}^{T-1}\frac{(\tilde{x}_{t+1} - \phi\tilde{x}_t - \bar{y}_t)^2}{2\sigma^2(1-\rho^2)}\right\} \\
&\propto\; \pi(\phi)\sqrt{1-\phi^2}\exp\left\{-\frac{(\phi-\mu_\phi)^2}{2\sigma_\phi^2}\right\},
\end{aligned}$$

where $\bar{y}_t = \rho\sigma(y_t - J_t Z_t)e^{-h_t/2}/\sqrt{\lambda_t}$,

$$\mu_\phi \;=\; \frac{\sum_{t=1}^{T-1}(\tilde{x}_{t+1} - \bar{y}_t)\tilde{x}_t}{s_x^2}, \quad \text{and} \quad \sigma_\phi^2 \;=\; \frac{\sigma^2(1-\rho^2)}{s_x^2},$$

with $s_x^2 = \rho^2\tilde{x}_1^2 + \sum_{t=2}^{T-1}\tilde{x}_t^2$. To sample from this conditional posterior distribution, we use the MH algorithm. We propose a candidate, $\phi^* \sim TN_{(-1,1)}(\mu_\phi, \sigma_\phi^2)$, where $TN_{(a,b)}(\mu, \sigma^2)$ denotes the normal distribution with mean μ and variance σ^2 truncated on the interval (a, b). Then, we accept it with probability

$$\min\left\{\frac{\pi(\phi^*)\sqrt{1-\phi^{*2}}}{\pi(\phi)\sqrt{1-\phi^2}},\, 1\right\}.$$

For the parameters, $\boldsymbol{\vartheta} \equiv (\sigma, \rho)$, there is no explicit distribution form which we can easily sample from. The conditional posterior density is given by

$$\begin{aligned}
\pi(\boldsymbol{\vartheta}\,|\,\cdot) \;&\propto\; (1-\rho^2)^{-\frac{T-1}{2}}\exp\left\{-\sum_{t=1}^{T}\frac{(y_t - \sqrt{\lambda_t} r_t e^{h_t/2} - J_t Z_t)^2}{2\lambda_t(1-\rho_t^2)e^{h_t}}\right\} \\
&\times\; \sigma^{-T}\exp\left\{-\frac{(1-\phi^2)\tilde{x}_1^2 + \sum_{t=1}^{T-1}(\tilde{x}_{t+1} - \phi\tilde{x}_t)^2}{2\sigma^2}\right\} \times \pi(\boldsymbol{\vartheta}),
\end{aligned}$$

where $\pi(\boldsymbol{\vartheta})$ is the prior density. We generate a candidate from the normal distribution based on the approximation of the posterior around the mode of the density. As an alternative way, we can generate (ϕ, σ, ρ) jointly by the MH algorithm with the posterior approximation around the mode, while we found that it is slightly less efficient than the separate generation of ϕ and (σ, ρ), which we recommend as described here.

Assuming the prior, $\mu \sim N(\mu_0, \sigma_{\mu 0}^2)$, we generate μ from its posterior density, $\mu \,|\, \cdot \sim N(\hat{\mu}, \hat{\sigma}_\mu^2)$, where

$$\begin{aligned} \hat{\sigma}_\mu^2 &= \left\{ \frac{1}{\sigma_{\mu 0}^2} + \frac{1-\phi^2}{\sigma^2} + \frac{(T-1)(1-\phi)^2}{(1-\rho^2)\sigma^2} \right\}^{-1}, \\ \hat{\mu} &= \hat{\sigma}_\mu^2 \left\{ \frac{\mu_0}{\sigma_{\mu 0}^2} + \frac{(1-\phi^2)x_1}{\sigma^2} + \frac{(1-\phi)\sum_{t=1}^{T-1}(x_{t+1} - \phi x_t - \rho\sigma\hat{e}_t)}{(1-\rho^2)\sigma^2} \right\}, \end{aligned}$$

and $\hat{e}_t = (y_t - J_t Z_t) e^{-h_t/2} / \sqrt{\lambda_t}$.

A.6 Jump parameters

For the jump parameters $\boldsymbol{\theta}_J$, the following priors are assumed: $\kappa \sim B(a_{\kappa 0}, b_{\kappa 0})$, $\mu_z \sim N(m_{y0}, c_{y0})$, and $\sigma_z^2 \sim IG(n_{y0}/2, S_{y0}/2)$. Then, the sample generation from the conditional posterior is as follows:

$$\kappa \,|\, \cdot \sim B(a_{\kappa 0} + T_J,\, b_{\kappa 0} + T - T_J),$$

where $T_J = \sum_{t=1}^T J_t$; and

$$\mu_z \,|\, \cdot \sim N(m_y^*,\, c_y^*), \qquad \sigma_z^2 \,|\, \cdot \sim IG(n_y^*/2, S_y^*/2),$$

where

$$\begin{aligned} c_y^* &= \left(\frac{1}{c_{y0}} + \frac{T_J}{\sigma_z^2} \right)^{-1}, \qquad m_y^* = c_y^* \left(\frac{m_{y0}}{c_{y0}} + \frac{\sum_{t=1}^T Z_t J_t}{\sigma_z^2} \right), \\ n_y^* &= n_{y0} + T_J, \quad \text{and} \quad S_y^* = S_{y0} + \sum_{t=1}^T (Z_t - \mu_z)^2 J_t. \end{aligned}$$

A.7 Seasonal- and announcement-effect parameters

We assume a prior, $v_\beta^2 \sim IG(n_{\beta 0}/2, S_{\beta 0}/2)$, and then simply generate the sample from its posterior: $v_\beta^2 \,|\, \cdot \sim IG(\hat{n}_\beta/2, \hat{S}_\beta/2)$, where

$$\hat{n}_\beta \;=\; n_{\beta 0} + K - 1, \qquad \hat{S}_\beta \;=\; S_{\beta 0} + \sum_{k=1}^{K-1} \frac{(\beta_{k+1} - \beta_k)^2}{c_k}.$$

The posterior generation of $v_{\alpha j}^2$ can be implemented in the same manner.

To generate the parameter φ_j in the announcement effect, we assume a prior denoted by $\pi(\varphi_j)$. The conditional posterior distribution of φ_j is given by

$$\pi(\varphi_j \,|\, \cdot) \;\propto\; \pi(\varphi_j) \exp\left\{ -\frac{(\varphi_j - \mu_{\varphi j})^2}{2\sigma_{\varphi j}^2} \right\},$$

where

$$\mu_{\varphi j} \;=\; \frac{\sum_{\ell=1}^{L-1} \alpha_{j\ell}\alpha_{j,\ell+1}}{\sum_{\ell=1}^{L-1} \alpha_{j\ell}^2}, \quad \text{and} \quad \sigma_{\varphi j}^2 \;=\; \frac{v_{\alpha j}^2}{\sum_{\ell=1}^{L-1} \alpha_{j\ell}^2}.$$

Using the MH algorithm, we propose a candidate, $\varphi_j^* \sim TN_{(-1,1)}(\mu_{\varphi j}, \sigma_{\varphi j}^2)$, and accept it with probability: $\min\{\pi(\varphi_j^*)/\pi(\varphi_j)\,, 1\}$.

A.8 Degree of freedom for Student-t distribution

The conditional posterior density of ν is

$$\pi(\nu \,|\, \cdot) \;\propto\; \pi(\nu) \prod_{t=1}^{T} \frac{((\nu-2)/2)^{\nu/2}}{\Gamma(\nu/2)} \lambda_t^{-\nu/2} \exp\left(-\frac{\nu - 2}{2\lambda_t} \right),$$

where $\pi(\nu)$ denotes the prior distribution. Following Watanabe (2001), we use the MH algorithm, where we generate a candidate from a normal distribution associated with the approximation around the mode of the posterior.

A.9 Parameters for RV measurement

For the parameters in the measurement equation of RV, (ξ, σ_u), the following priors are assumed: $\xi \sim N(\xi_0, q_0^2)$, and $\sigma_u^2 \sim IG(n_{u0}/2, S_{u0}/2)$. Define $W_\tau = \log \sum_{t \in D(\tau)} \exp(h_t)$.

We generate ξ and σ_u from the conditional posterior distribution: $\xi \,|\, \cdot \sim N(\hat{\xi}, \hat{q}^2)$, $\sigma_u^2 \,|\, \cdot \sim IG(\hat{n}_u/2, \hat{S}_u/2)$, respectively, where

$$\begin{aligned} \hat{q}^2 &= \left(\frac{1}{q_0^2} + \frac{N}{\sigma_u^2} \right)^{-1}, \qquad \hat{\xi} = \hat{q}^2 \left(\frac{\xi_0}{q_0^2} + \frac{\sum_{\tau=1}^{N} \{\log(\mathrm{RV}_\tau) - W_\tau\}}{\sigma_u^2} \right), \\ \hat{n}_u &= n_{u0} + N, \quad \text{and} \quad \hat{S}_u = S_{u0} + \sum_{\tau=1}^{N} \{\log(\mathrm{RV}_\tau) - \xi - W_\tau\}^2 . \end{aligned}$$

References

Andersen, T. and L. Benzoni (2009). Realized volatility. In A. T., R. Davis, J. Kreiss, and T. Mikosch (Eds.), *Handbook of Financial Time Series*, pp. 555–575. Berlin: Springer Verlag.

Andersen, T., T. Bollerslev, and F. Diebold (2007). Roughing it up: including jump components in the measurement, modeling, and forecasting of return volatility. *Review of Economics and Statistics 89*, 701–720.

Andersen, T., T. Bollerslev, and F. Diebold (2010). Parametric and nonparametric volatility measurement. In Y. Aït-Sahalia and L. P. Hansen (Eds.), *Handbook of Financial Econometrics*, pp. 67–138. Amsterdam: North Holland.

Barndorff-Nielsen, O. E. and N. Shephard (2004). Power and bipower variation with stochastic volatility and jumps. *Journal of Financial Econometrics 2*, 1–37.

Barndorff-Nielsen, O. E. and N. Shephard (2006). Econometrics of testing for jumps in financial economics using bipower variation. *Journal of Financial Econometrics 4*, 1–30.

Barndorff-Nielsen, O. E. and N. Shephard (2007). Variation, jumps and high-frequency data in financial econometrics. In R. Blundell, P. Torsten, and W. K. Newey (Eds.), *Advances in Economics and Econometrics. Theory and Applications, Ninth World Congress*, pp. 328–372. Cambridge, UK: Cambridge University Press.

Bekierman, J. and B. Gribisch (2021). A mixed frequency stochastic volatility model for intraday stock market returns. *Journal of Financial Econometrics 19*(3), 496–530.

Chib, S. (2001). Markov chain Monte Carlo methods: computation and inference. In J. J. Heckman and E. Leamer (Eds.), *Handbook of Econometrics*, Volume 5, pp. 3569–3649. Amsterdam: North-Holland.

Chib, S., F. Nardari, and N. Shephard (2002). Markov chain Monte Carlo methods for stochastic volatility models. *Journal of Econometrics 108*, 281–316.

Corsi, F., D. Pirino, and R. Renò (2010). Threshold bipower variation and the impact of jumps on volatility forecasting. *Journal of Econometrics 159*, 276–288.

de Jong, P. and N. Shephard (1995). The simulation smoother for time series models. *Biometrika 82*, 339–350.

Doornik, J. (2006). *Ox: Object Oriented Matrix Programming*. London: Timberlake Consultants Press.

Eraker, B., M. Johanners, and N. G. Polson (2003). The impact of jumps in returns and volatility. *Journal of Finance 53*, 1269–1330.

Geweke, J. (1992). Evaluating the accuracy of sampling-based approaches to the calculation of posterior moments. In J. M. Bernardo, J. O. Berger, A. P. Dawid, and A. F. M. Smith (Eds.), *Bayesian Statistics*, Volume 4, pp. 169–188. New York: Oxford University Press.

Ghysels, E., A. C. Harvey, and E. Renault (2002). Stochastic volatility. In C. R. Rao and G. S. Maddala (Eds.), *Statistical Methods in Finance*, pp. 119–191. Amsterdam: North-Holland.

Giacomini, F. and H. White (2006). Tests of conditional predictive ability. *Econometrica 74*, 1548–1578.

Hansen, P., A. Lunde, and J. Nason (2011). The model confidence set. *Econometrica 79*, 453–497.

Hansen, P. R. and A. Lunde (2005). A forecast comparison of volatility models: does anything beat a GARCH (1, 1)? *Journal of Applied Econometrics 20*, 873–889.

Kim, S., N. Shephard, and S. Chib (1998). Stochastic volatility: likelihood inference and comparison with ARCH models. *Review of Economic Studies 65*, 361–393.

Koopman, S. J. and M. Scharth (2012). The analysis of stochastic volatility in the presence of daily realized measures. *Journal of Financial Econometrics 11*, 76–115.

Nakajima, J. (2017). Bayesian analysis of multivariate stochastic volatility with skew distribution. *Econometric Reviews 36*, 546–562.

Nakajima, J. and Y. Omori (2009). Leverage, heavy-tails and correlated jumps in stochastic volatility models. *Computational Statistics and Data Analysis 53*, 2535–2553.

Omori, Y., S. Chib, N. Shephard, and J. Nakajima (2007). Stochastic volatility with leverage: fast likelihood inference. *Journal of Econometrics 140*, 425–449.

Omori, Y. and T. Watanabe (2008). Block sampler and posterior mode estimation for asymmetric stochastic volatility models. *Computational Statistics and Data Analysis 52*, 2892–2910.

Patton, A. J. (2011). Volatility forecast comparison using imperfect volatility proxies. *Journal of Econometrics 160*, 246–256.

Pitt, M. and N. Shephard (1999). Filtering via simulation: auxiliary particle filter. *Journal of the American Statistical Association 94*, 590–599.

Prado, R. and M. West (2010). *Time Series Modeling, Computation, and Inference*. New York: Chapman & Hall/CRC.

Santos, A. (2019). High-frequency volatility in a time deformed framework, the role of volume, durations and jumps through intraday data. *Computational Economics*, in press.

Shephard, N. (1996). Statistical aspects of ARCH and stochastic volatility. In D. V. Hinkley and O. E. Barndorff-Nielsen (Eds.), *Time Series Models in Econometrics, Finance and Other Fields*, pp. 1–67. London: Chapman & Hall.

Shephard, N. (2005). *Stochastic Volatility: Selected Readings*. Oxford: Oxford University Press.

Shephard, N. and M. Pitt (1997). Likelihood analysis of non-Gaussian measurement time series. *Biometrika 84*, 653–667.

Stroud, J. R. and M. S. Johannes (2014). Bayesian modeling and forecasting of 24-hour high-frequency volatility. *Journal of the American Statistical Association 109*, 1368–1384.

Takahashi, M., Y. Omori, and T. Watanabe (2009). Estimating stochastic volatility models using daily returns and realized volatility simultaneously. *Computational Statistics and Data Analysis 53*, 2404–2426.

Takahashi, M., T. Watanabe, and Y. Omori (2016). Volatility and quantile forecasts by realized stochastic volatility models with generalized hyperbolic distribution. *International Journal of Forecasting 32*, 437–457.

Takahashi, M., T. Watanabe, and Y. Omori (2021). Forecasting daily volatility of stock price index using faily returns and realized volatility. *Econometrics and Statistics*, in press.

Watanabe, T. (2001). On sampling the degree-of-freedom of Student's-t disturbances. *Statistics and Probability Letters 52*, 177–181.

Watanabe, T. and Y. Omori (2004). A multi-move sampler for estimating non-Gaussian time series models: Comments on Shephard & Pitt (1997). *Biometrika 91*, 246–248.